Physicochem. Probl. Miner. Process. 50(2), 2014, 535−550

www.minproc.pwr.wroc.pl/journal/

Physicochemical Problems of Mineral Processing

ISSN 1643-1049 (print)
ISSN 2084-4735 (online)

Received September 17, 2013; reviewed; accepted November 25, 2013

INVESTIGATION ON DIFFERENT BEHAVIOR AND MECHANISM OF Ca(II) AND Fe(III) ADSORPTION ON SPODUMENE SURFACE

Fushun YU, Yuhua WANG, Jinming WANG, Zhenfu XIE

School of Minerals Processing and Bioengineering, Central South University, Changsha 410083, China, csuwangyh@163.com

Abstract: Behavior and mechanism of Ca^{2+} and Fe^{3+} adsorption on spodumene surface were investigated by micro flotation tests, zeta potential measurements, and density functional theory (DFT) calculation methods. The micro flotation tests showed that Ca^{2+} and Fe^{3+} activated the flotation of spodumene remarkably. However, the effect of Fe^{3+} was more significant than that of Ca^{2+}. Additionally, Fe^{3+} significantly changed the zeta potential of spodumene while Ca^{2+} showed a little change. Meanwhile, the calculated adsorption energy of Fe^{3+} on spodumene surface was much greater than that of Ca^{2+} indicating that Fe^{3+} is more apt to be adsorbed on spodumene surface than Ca^{2+}. The value of bond population in Ca-O illustrated that the bond of Ca-O consists of partial covalent proportion and some ionic component. On the contrary, the bond of Fe-O showed a relatively strong covalent property. The partial density of states (PDOS) of free Ca/Fe and the reacted O atom on spodumene (110) surface before and after the adsorption showed that Fe 3d orbital and O 2p orbital formed hybridization. The density of states (DOS) near the Fermi level of spodumene surface after adsorption with Fe^{3+} was much stronger than that with Ca^{2+}.

Keywords: *spodumene surface, calcium ions, iron ions, adsorption mechanism, DFT calculation*

Introduction

Spodumene ($LiAl(SiO_3)_2$) is a typical pyroxene mineral consisting of lithium aluminium chain silicate containing approximately 8% Li_2O. It is the richest lithium bearing minerals in nature. In the past time, the major consumer of spodumene was the aluminum and ceramics industry (Wendt 1971; Nicholson 1978). However, a great number of applications of spodumene and lithium compounds are being developed rapidly in the battery and fuel cell industry (Landgrebe and Nelson 1976; Cooper and Borg 1976; Burns and Nelson 1978).

In the crystal model of spodumene, silicates tetrahedron $[SiO_3]^{2-}$ are represented by the chains of tetrahedron which are bound together laterally through the ionic bonding

http://dx.doi.org/10.5277/ppmp140210

with Li and Al in octahedral coordination. The irregular six coordination of Li^+ and Al^{3+} with oxygen are indicated by the octahedral linking the silicate tetrahedral chains (Bragg and Claringbull 1965). Aluminum is in octahedral coordination with six oxygen including two non-bridging basal oxygen and four apical oxygen. Lithium in spodumene coordinates with six oxygen which consist of two non-bridging basal oxygen, two bridging basal oxygen, and two apical oxygen (Zachariasen 1963; Bloss 1971; Kwang and Douglas 2003). Spodumene has a very pronounced cleavage plane (110), which results in typically lath-shaped particles on breaking (Krause 1968). The Si-O bond in spodumene crystallographic structure mainly possesses covalent component, the average length of which is 0.158 nm while the bond of Li-O and Al-O has obvious ionic features. The average bond length of Li-O is 0.221 nm, and for Al-O the value is 0.192 nm. The calculated ionic component of Li-O bond is 79.81%, the ionic component of Al-O bond is 64.30 %, according to the Pauling empirical formula (Chuanyao and Wanzhong 2001). Therefore, the bond strength of Li-O is relatively weak and disaggregation of spodumene would occur mainly alone the broken directions of Li-O bond. The exposed ions on the disaggregated surface of spodumene will be Li, a bit of Si and Al, which has been verified by the investigation results of X-ray photoelectron spectroscopy (XPS) (Chuanyao and Wanzhong 2001). The occurrence of ion exchange makes H^+ in the liquid replace the Li^+ on the mineral surface. H^+ ions are adsorbed on the oxygen districts of the mineral surface while the Si and Al districts adsorb OH^-. Consequently, a large quantity of hydroxyl are bonded on the surface of spodumene, which leads to the negative charge of spodumene surface on a wide range of pH value, in other words, the point of zero charge of spodumene is very low. This explains the reason of the floatability of spodumene is bad by using anionic collectors, e.g., sodium oleate, and turns good with cationic collectors, e.g. lauryl amine.

In the flotation practice of industry, spodumene is activated by the presence of Ca^{2+} and Fe^{3+} which derives from operating water and iron balls in the mill. Floatability of the activated spodumene enhances greatly as anionic collectors are adopted. In this paper, effects of Ca^{2+} and Fe^{3+} ions on the flotation behavior of spodumene were investigated by pure minerals micro-flotation tests. The zeta potential measurements were carried out to reveal the charge changing on the mineral surface. The adsorption of Ca^{2+} and Fe^{3+} ions on spodumene (110) surface was simulated by the density functional theory (DFT), which was an attempt to display the mechanisms of the interaction of Ca/ Fe and spodumene surface by means of microscopic quantum chemical calculations.

Materials and methods

Materials

A pegmatic spodumene ore was obtained from the Keketuohai Rare Metal Mine located in the Xinjiang Altay district. The hand-picked high-grade spodumene sample

was first crushed with hammer, then ground in a porcelain mill with agate balls in it, and finally screened with stainless steel screens. The sample was immersed in HCl of 3% concentration for 30 min to eliminate the impurities on the mineral surface. The processed sample was washed repeatedly using distilled water until the pH of the supernatant reached natural level. Subsequently, the -0.105+0.038 mm and -0.038 mm samples were filtered, vacuum-dried, and stored in glass bottles for the flotation tests and measurements.

Spodumene sample used in this study was a fairly pure crystal with a bit of Fe, Na, K, Ca, etc. as impurities as presented in Table 1.

Table 1. Chemical compositions of spodumene sample (%)

Li_2O	Al_2O_3	SiO_2	Fe_2O_3	Na_2O	K_2O	CaO	MnO	P_2O_5	BeO	Ta_2O_5	Nb_2O_5
7.81	25.99	62.74	0.54	0.312	0.156	0.36	0.127	0.16	0.028	0.019	0.028

The infrared spectrum of spodumene sample is shown in Fig. 1. The characteristic marked peaks in Fig. 1 meet well with the standard peaks of spodumene (Wenshi Peng and Gaokui Liu 1982), which also indicates that spodumene sample possesses a high purity.

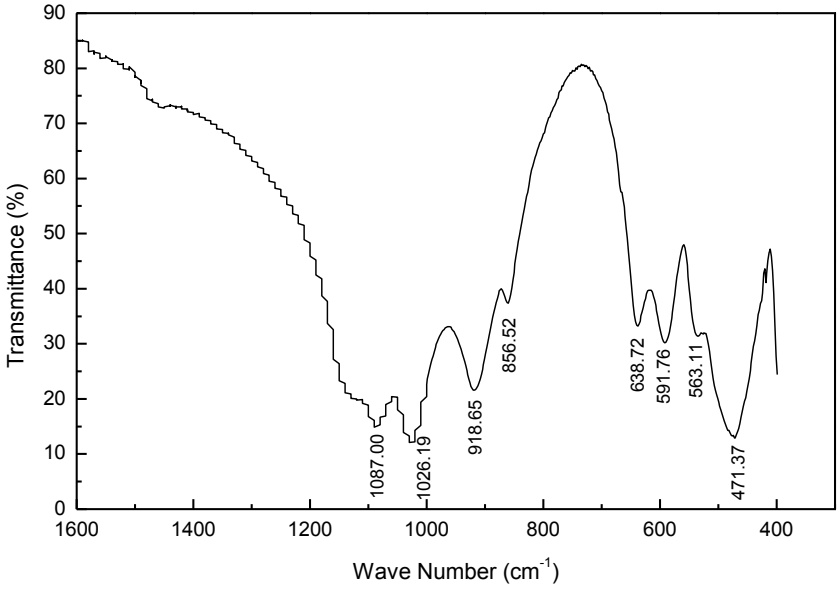

Fig. 1. Infrared spectra of spodumene sample

Sodium oleate of analytical quality was used as a collector for the micro-flotation tests while $FeCl_3 \cdot 6H_2O$ and $CaCl_2$ of analytical quality were used as activators. The solutions of HCl and NaOH were used to adjust the pH of the system.

Methods

Micro flotation tests

The micro flotation tests were performed in a laboratory flotation apparatus using -0.105+0.038 mm spodumene sample as a feed. At each test, 5 g of sample was placed in a plexiglass cell (40 cm^3), which was then filled with distilled water. The pH was adjusted to the target value before adding the individual flotation reagents. The sample was conditioned for 2 min after the reagent adding each, and the flotation time was kept as 5 min. All flotation tests were carried out at room temperature around 25 ^oC. The concentrate and tailings were filtered, dried, and weighed to calculate the flotation recovery of spodumene under various flotation conditions.

Zeta potential measurements

The zeta potentials of the sample were measured using a Brookhaven Zeta plus zeta meter (USA). The sample was ground to 0～5 μm in an agate mortar by hand. A 0.05 g of sample was placed in a 100 cm^3 breaker, stirred for 15 min with 80 cm^3 distilled water and reagents. Next, the pH was adjusted and measured. The results presented in this paper are the average of three independent measurements with a typical variation of ±2 mV. Repeated tests showed that the conditioning procedure was reasonable and credible.

Computational methods

The geometry optimizations were performed using Cambridge Serial Total Energy Package (CASTEP), developed by Payne et al. (1992), which is a first-principle pseudopotential method based on Density-Functional Theory (DFT). The DFT calculations employing plane wave (PW) basis sets and ultrasoft pseudopotentials were performed (Perdew and Wang 1992; Vanderbilt 1990). The exchange correlation functional used was the generalized gradient approximation (GGA) developed by Perdew, Burke and Ernzerhof (PBE) (Perdew and Burke 1996). The interactions between valence electrons and the ionic core were represented by ultrasoft pseudopotentials. The computations were based on spodumene structure where space group is *C*2/*c* (15). The valence electron configurations considered in the study included Ca 3p6 4s2, Fe 3p6d6 4s2, O 2s2p4, Li 2s1, Al 3s2 p1, Si3s2 p2. The kinetic energy cut-off of 260 eV for the plane wave basis was used throughout the study, and the Brillouin zone was sampled using Monkhorst and Pack special k-points of a 1×2×3 grid for surface calculation (Monkhorst and Pack 1976), which shows that the cut-off energy and the k-point meshes are sufficient for the system. For self-consistent

electronic minimization, the Pulay Density Mixing method was employed with a convergence tolerance of $2.0 \cdot 10^{-6}$ eV/atom. The convergence criteria for structure optimization and energy calculation met the conditions of (a) an energy tolerance of $2 \cdot 10^{-5}$ eV/atom; (b) maximum force tolerance of 0.05 eV/Å; and (c) maximum displacement tolerance of 0.002 Å.

After testing the slab thickness and vacuum slab thickness, a 2×2×1 perfect spodumene (110) surface using super-cell geometries with 3 atomic layers and 10 Å vacuum slab was modeled. The outermost atomic layer of the substrate was allowed to relax while the two bottommost atomic layers of the substrate were fixed to the bulk coordinates in the adsorption calculations. The optimizations of Ca and Fe atoms were calculated in a 10×10×10 Å cubic cell and the optimizations were performed at the gamma point in the Brillouin zone. The optimized lattice parameters of perfect spodumene are a=9.486 Å, b=8.237 Å, c= 5.152 Å, β=110.74 °, which are very close to the experimental values (Joan et al. 1969) of a=9.449 Å, b=8.386 Å, c= 5.213 Å, β=110.10°. These values indicate that the calculated results agree well with experimental data.

Results and discussion

Results

Micro-flotation of spodumene

The micro-flotation tests were conducted to show flotation behavior of spodumene and the activation of Ca^{2+} and Fe^{3+} as a function of solution pH. Sodium oleate was used as a collector in these tests at the concentration of $7 \cdot 10^{-4}$ M. Calcium chloride and ferric chloride were used as an activator at the concentration of $1.2 \cdot 10^{-3}$ M and $1.5 \cdot 10^{-4}$ M, respectively. As seen from Fig. 2, the natural floatability of spodumene was poor, and the highest recovery was under 10% at the whole pH range. Ca^{2+} and Fe^{3+} activated the flotation of spodumene. In addition, the recovery reached to over 70% in a strong alkaline pH range when the mineral was activated with Ca^{2+}. On the contrary, the highest recovery of spodumene reached as high as 95% in the pH range of 7-9 after the activation with Fe^{3+}. It is interesting to note that the flotation recovery of spodumene activated by Fe^{3+}decreased largely in alkaline pH range of exceeding 9. The rational explanation is that the adsorption of Fe^{3+} ions on the surface of spodumene made negative ions easier to interact with the mineral surfaces. A competitive adsorption occurred between the anionic collectors and OH^- ions in the solution. At acidic and neutral pH values, the anionic collectors preferentially adsorbed on the activated mineral surface while in strong alkaline pH range the activity of OH^- ions was more than that of anionic collector. The OH^- ions prior adsorbed on the mineral surface caused a decrease in the flotation recovery in alkaline pH range. It is also noteworthy that the effective dosages of Ca^{2+} and Fe^{3+} are fairly different because the effective concentration of Fe^{3+} is nearly one-tenth of Ca^{2+}, which

implies the adsorption of Fe^{3+} on spodumene surface was more efficient than that of Ca^{2+}. Figures 3 and 4 illustrate this further.

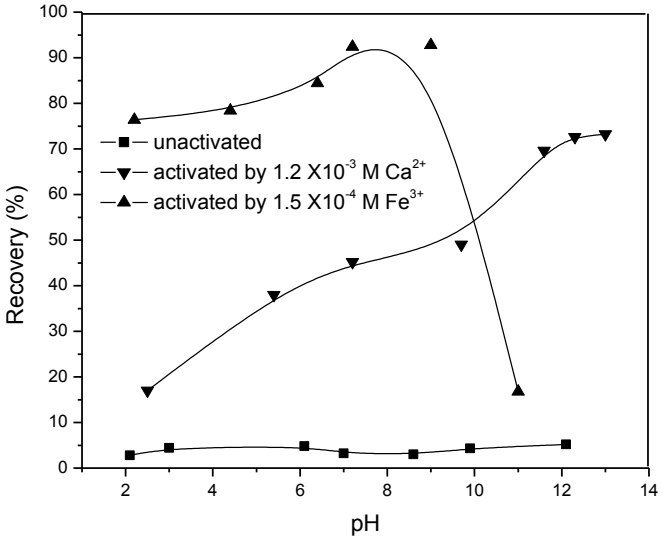

Fig. 2. Flotation recovery of spodumene as a function of pH in $7 \cdot 10^{-4}$ M sodium oleate solution

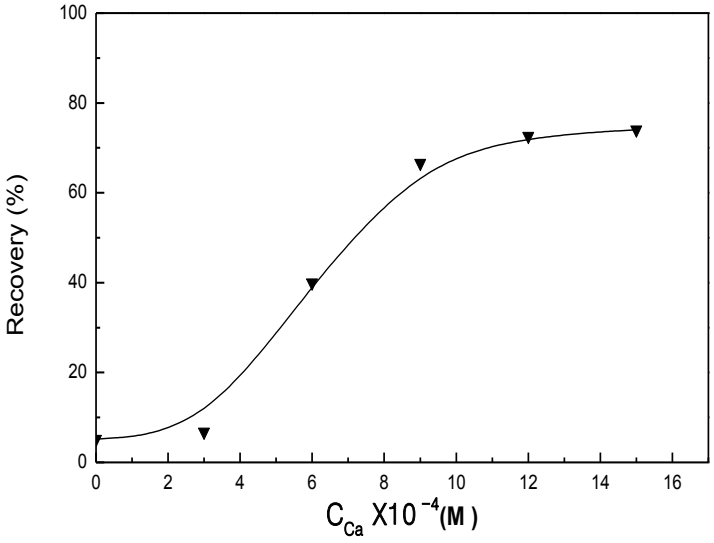

Fig. 3. Flotation recovery of spodumene as a function of Ca^{2+} dosage in $7 \cdot 10^{-4}$ M sodium oleate solution at pH 12.3±0.15

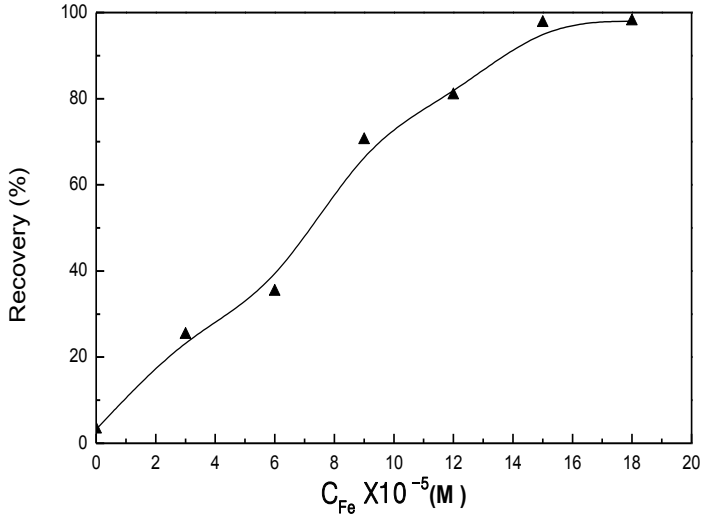

Fig. 4. Flotation recovery of spodumene as a function of Fe^{3+} dosage in $7 \cdot 10^{-4}$ M sodium oleate solution at pH7.5±0.15

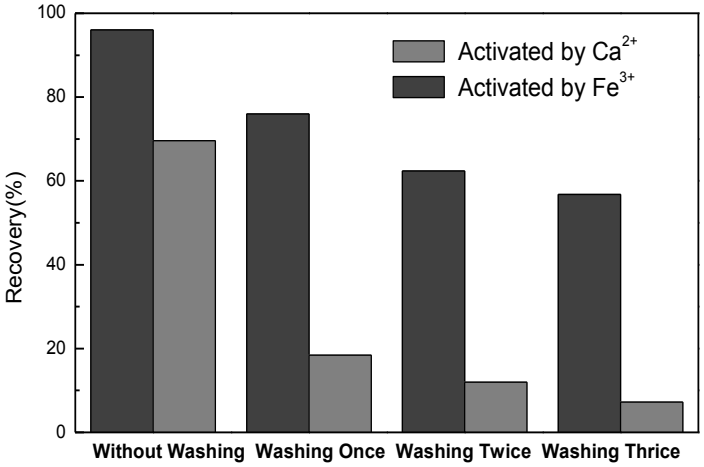

Fig. 5. Effect of washing on the flotation of spodumene activated by Ca^{2+}, Fe^{3+}

The washing tests were also carried out to investigate the effect of Ca^{2+} and Fe^{3+} adsorption on spodumene surface. In this test work, spodumene sample was first activated by Ca^{2+} or Fe^{3+}, then the pulp was precipitated for 1 min, and the upper liquid was decanted, then distilled water was added into the pulp, and agitated for 1 min. The pulp was also precipitated for 1 min, and the upper liquid was decanted again. This procedure is called ‘washing once’. Repeating this procedure one gets ‘washing twice’, ‘washing thrice’, and so on. In the activation tests, calcium chloride

was used at a dosage of $1.2 \cdot 10^{-3}$ M at a pH of 12.3±0.15, and ferric chloride was used at a dosage of $1.5 \cdot 10^{-4}$ M at a pH of 7.5±0.15. After the washing process, the flotation was carried out using sodium oleate as collector at a dosage of $7 \cdot 10^{-4}$ M. The results are shown in Fig. 5.

It can be seen from Fig. 5 that flotation of spodumene decreased rapidly after the washing when it was activated by Ca^{2+}, the flotation recovery declined to a non-activated level after the washing thrice. In contrast, the influence of the washing on the floatability of spodumene was not so notable when the mineral was activated by Fe^{3+}. These results showed that the adsorption of Fe^{3+} on spodumene was more firm than that of Ca^{2+}.

Zeta potential measurement

The electrophoretic mobility of spodumene in absence and in the presence of Ca^{2+}/Fe^{3+} was measured, and the results are shown in Fig. 6. The zeta potential of spodumene follows the general trend of other silicate minerals. The point of zero charge (PZC) of spodumene was found to be pH of about 2.68. The surface charge of spodumene was negative at pH range of 3 to 12. This result is agreed with the results by other researchers (Fuerstenau and Pradip 2005). Figure 6 also shows the effect of Ca^{2+}/Fe^{3+} on the zeta potential of spodumene. The zeta potentials of spodumene slightly shifted towards positive values in the presence of Ca^{2+} and the pzc of spodumene shifted slightly to the alkaline pH value of about 3.3 as well. This indicates that the adsorbed Ca^{2+} ions

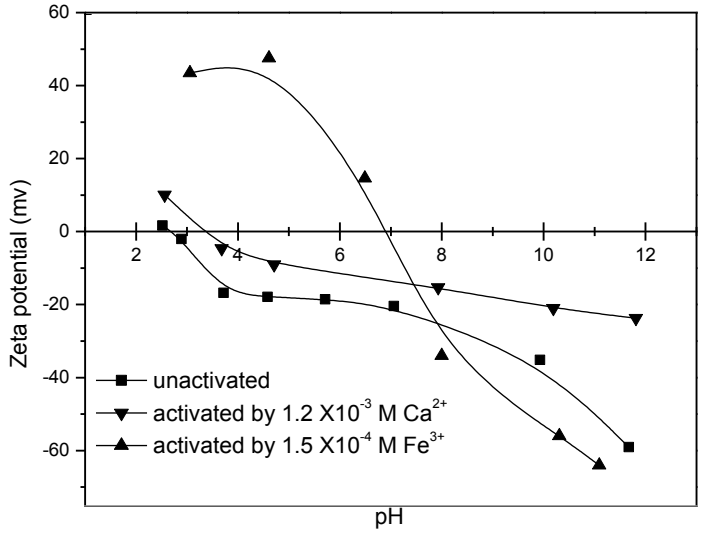

Fig. 6. Zeta potential of spodumene vs. pH in absence and in the presence of Ca^{2+}/Fe^{3+}

may lie closer to the outer stern planes of the electrical double layer of the mineral. It can be said that this adsorption is mainly by electrostatic attraction. However, the zeta potentials of spodumene showed a pronounced shift to positive values in presence of Fe^{3+}, the PZC of the sample shifted largely to alkaline pH value of about 6.9. It can be deduced that the adsorbed Fe^{3+} ions may lie on the inner stern planes of the electrical double layer. The adsorption can be attributed to chemical adsorption or specific adsorption. It is also worth noting that the zeta potentials of spodumene turn greatly to much negative values in alkaline pH range in the presence of Fe^{3+}. This phenomenon may be caused by the liable adsorption of OH^- ions on the surface of the mineral via the already adsorbed Fe^{3+} ions in alkaline pH values.

DFT calculation results

The electronic structure and properties of spodumene (110) surfaces and the super-cell model of spodumene (110) surface is shown in Fig. 7.

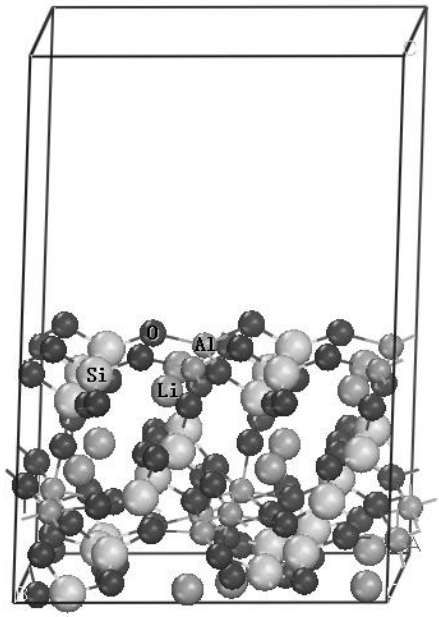

Fig. 7. The slab models of spodumene (110) surface

The analysis of density of states (DOS) could give an insight into the surface properties of the mineral at an electronic level. The partial DOS of the perfect spodumene (110) surface was calculated by the CASTEP module and the Fermi energy was set at 0 eV ($E_f = 0$) in the DOS curve is shown in Fig. 8. As seen in Fig. 8, there are mainly two kinds of oxygen: non-bridging basal oxygen and bridging basal oxygen, which were marked as O1 and O2 respectively. The valence bands of spodumene (110) surface are extended down to approximately -22 eV below the Fermi

level (E_f). The whole valence bands could be divided into two parts: the upper valence band between -10 eV and 0 eV and the deep level of valence band between -22 eV and -15.5 eV. The conduction band consists of the Al 3s and Al 3p orbital, together with the Li 2s orbital. It is known that electrons near the Fermi level have a strong activity and physical or chemical reactions usually occur around Fermi level. The reactivity of a certain atom can be judged from the composition of the DOS around the Fermi level. It can be seen that Li and Al has little contribution to the DOS around the Fermi level, which indicates the activity of Li and Al are weak, and it is hard to act as active sites for the absorption of anionic collectors, e.g., sodium oleate on spodumene surface. This conclusion is consistent with the previous flotation test results.

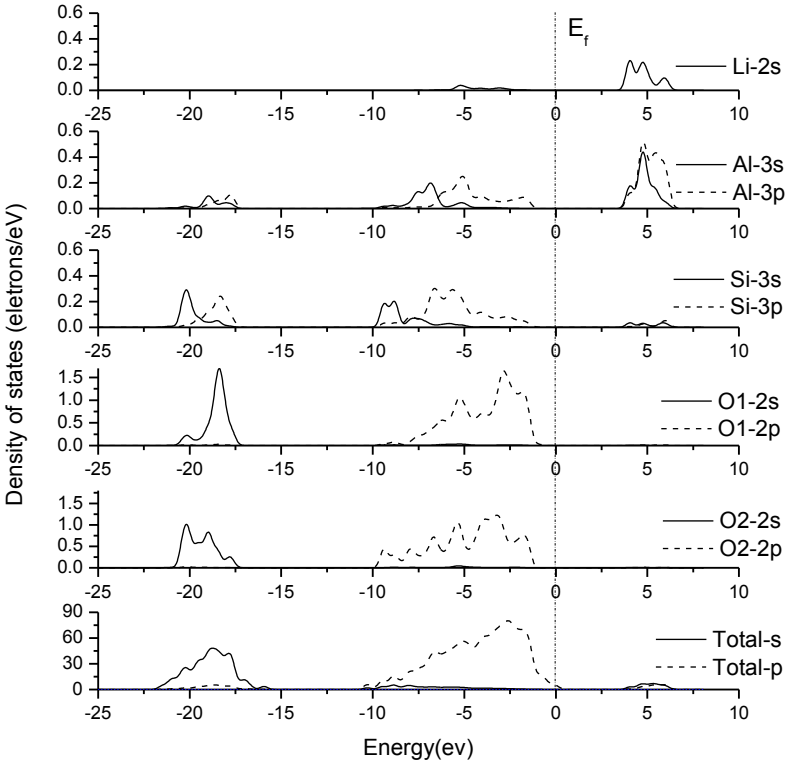

Fig. 8. PDOS of Li, Al, Si, O atoms on spodumene (110) surface

Adsorption of Ca/Fe on spodumene (110) surface

After the geometry optimization, Ca/Fe was positioned on spodumene (110) surface at various possible adsorption sites. For the feasibility and validity of calculation by CASTEP, Ca/Fe was set as uncharged. Particularly, Ca, Fe atoms were substituted for Ca^{2+}, Fe^{3+} respectively in the simulate adsorption calculation.

The adsorption energy of Ca or Fe atoms on different adsorption sites can be expressed by Eq. 1 (Kazume et al. 2008; Reuter and Scheffler 2001):

$$\Delta E = E_{\text{slab+adsorbate}} - E_{\text{slab}} - E_{\text{adsorbate}} \quad (1)$$

where $E_{\text{slab+adsorbate}}$ E_{slab} represent the total energies of spodumene model before and after Ca^{2+}/Fe^{3+} adsorption, respectively. $E_{\text{adsorbate}}$ represents the calculated energy of Ca/Fe atom and ΔE represents the adsorption energy of Ca/Fe atom. More negative value of ΔE indicates that the adsorption reaction of Ca^{2+}/Fe^{3+} occurs more readily.

Using a perfect spodumene (110) surface, various initial structures were generated for the adsorption of Ca/Fe atom on the O atoms. It was found that Ca/Fe atom was voluntarily close to the bridge site between two non-bridging basal O atoms after geometry optimization. This observation indicates that the bridge site between two non-bridging basal O atoms on spodumene (110) surface is the most stable position for the adsorption of Ca/Fe atom. The optimized configurations of the adsorption of Ca/Fe atom on spodumene surface are shown in Fig. 9.

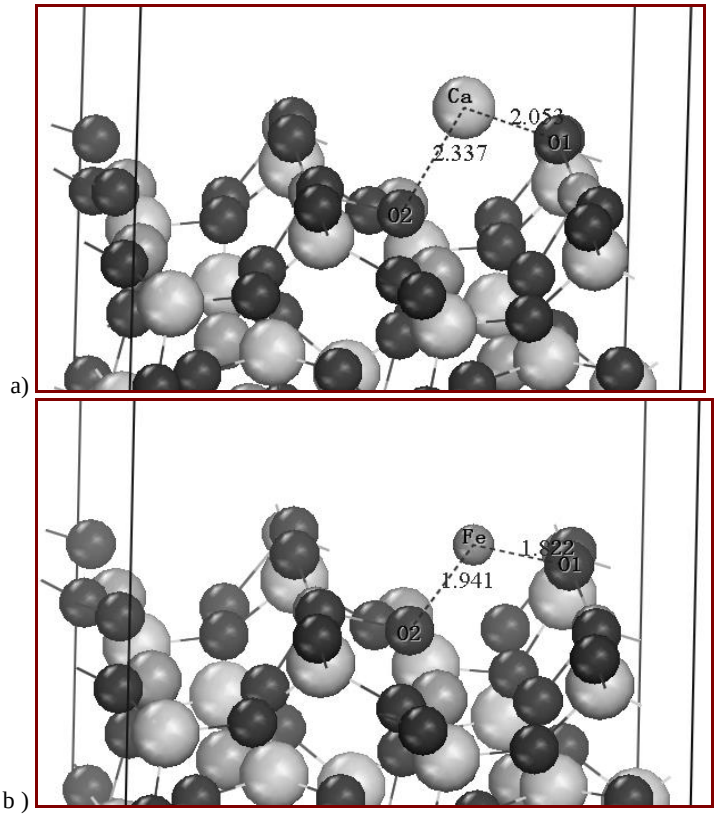

Fig. 9 (a) Adsorption of Ca atom on spodumene (110) surface
(b) Adsorption of Fe atom on spodumene (110) surface

As shown in Fig. 9, the bond lengths of Ca-O1 and Ca-O2 are 0.2053 nm (2.053 Å) and 0.2337 nm (2.337 Å), respectively. These values are bigger than that of Fe-O where 1.822 Å and 1.941 Å values were obtained for Fe-O1 and Fe-O2. Additionally, the adsorption energy of Fe on spodumene surface was calculated as -369.00 kJ/mol which is much greater than that of Ca as -187.14 kJ/mol. This illustrates further that Fe is more apt to be adsorbed on spodumene surface and the combination is more firm than Ca.

Bond population analysis schemes implemented in CASTEP were used to determine the strength of the bonds in the observed multi atomic complexes. Its values, on a scale from -1 to 1, represent a bonding state when the overlap population values are positive and anti-bonding state when the values are negative. The values with zero overlap indicate no significant interaction occurred between two atoms (Segall et al. 1996). Besides bonding states, covalence of the bond can also be determined since it is proportional to the overlap population. Therefore, the closer the bond population to 1, the more covalent the bond is between the atoms. Relative overlap population between two atoms would indicate the degree of covalence of the bond. Furthermore, iconicity of the bond can be indicated from the effective mulliken charges on the participating atoms. A Mulliken population analysis, while not giving realistic charges at individual lattice atom sites, is a valuable tool for comparing changes in charge between one lattice atom and another (Von et al. 2007). The calculated atomic populations in Ca, Fe and O, and the bond population in Ca-O and Fe-O bonds are presented in Table 2.

Table 2. Mulliken atomic population and charge on Ca, Fe, O and Mulliken bond population analysis

Mulliken Atom Population						Bond Population Analysis		
Atom	s	p	d	Total	Charge(e)	Bond	Bond population	Bond length(Å)
Ca	2.68	5.99	0.57	9.24	0.76	Ca-O1	0.09	2.053
Fe	0.46	0.05	7.12	7.63	0.37	Ca-O2	0.02	2.337
O1 (absorbed with Ca)	1.87	5.19	0	7.06	–1.06	Fe-O1	0.25	1.822
O2 (absorbed with Ca)	1.86	5.32	0	7.18	-1.18	Fe-O2	0.17	1.941
O1 (absorbed with Fe)	1.87	5.11	0	6.98	-0.98			
O2 (absorbed with Fe)	1.85	5.24	0	7.09	-1.09			

As seen in Table 2 that the bond populations in Ca-O1 and Ca-O2 are 0.09 and 0.02, respectively, indicating the covalent proportion in the bond of Ca-O1 and Ca-O2 are very weak. Moreover, the effective charge on Ca (+0.76 e) and O (-1.06/-1.18 e) shows the existence of ionic bonds between Ca atom and O atoms. On the contrary,

the bond populations in Fe-O1 and Fe-O2 are 0.25 and 0.17, respectively, indicating that a steady covalent bond of Fe-O is formed after the Fe atom adsorption on spodumene surface.

The analysis of density of states

The PDOS of free Ca/Fe and the reacted O atom on spodumene (110) surface before and after the adsorption are shown in Figs.10 and 11.

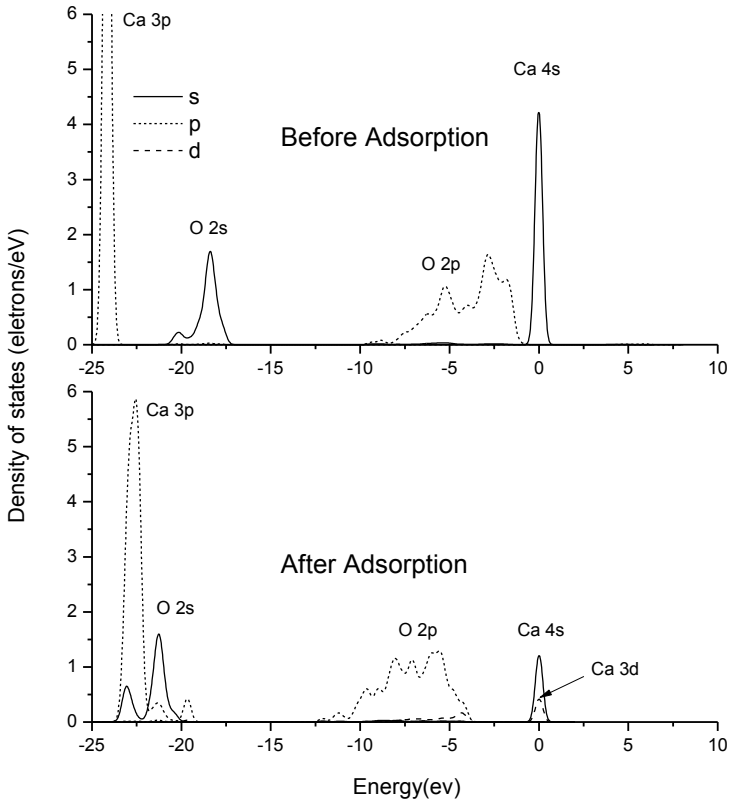

Fig. 10. PDOS of Ca and O on spodumene (110) surface before and after the adsorption between them

For free Ca^{2+} before adsorption, the state of Ca 3p orbital is located at -23 eV to -25 eV; and the state of Ca 4s orbital lies at the Fermi level (E_f = 0), indicating a certain activity of the free Ca^{2+}. After the adsorption on spodumene surface, the state peak of Ca 4s orbital reduced largely, and the peak value of 3p state moved to the higher energy level. For the O atom on spodumene surface, which reacts with the Ca atom, the PDOS of the O 2s and O 2p shift to the lower energy level after the adsorption.

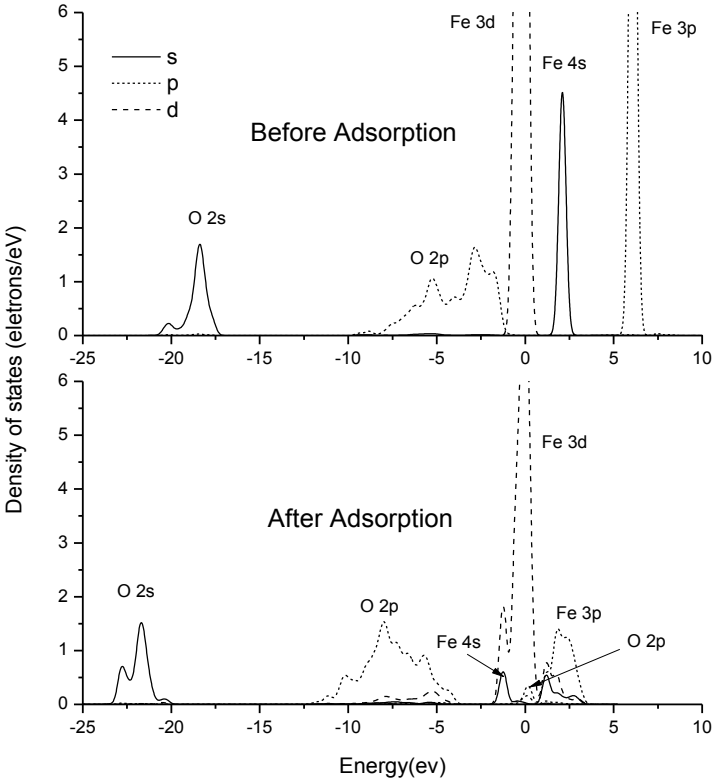

Fig. 11. PDOS of Fe and O on spodumene (110) surface before and after the adsorption between them

The PDOS of free Fe atom consists of Fe 3d orbital at the Fermi level, Fe 4s and Fe 3p orbital at the conduction band. After adsorption on spodumene surface, the PDOS of Fe changes apparently. The state peak of Fe 3d orbital reduces. Meanwhile, the Fe 4s state moves to the valence band, and the peak of which deceases; the peak value of Fe 3p shifts from -6 eV to -2 eV. In addition, the peaks of Fe 3d orbital and O 2p orbital are overlapped at the Fermi level (E_f = 0), implying a strong hybridization between them has formed. In other words, the adsorption of Fe^{3+} on spodumene surface is a steady chemical adsorption, as confirmed from the analysis of Table 2.

It is worthy to note that the DOS near the Fermi level of spodumene surface after adsorption with Fe^{3+} is much stronger than that with Ca^{2+}, which implies that the activity of the adsorbed Fe^{3+} on the mineral surface is greater than that of Ca^{2+}. This conclusion is also verified by the previous flotation tests.

Conclusions

The micro flotation tests showed that the natural flotation of spodumene is poor in the presence of anionic collectors. The results showed that Ca^{2+} and Fe^{3+} can remarkably activate the flotation, among which, Fe^{3+} displayed a more superior performance compared to Ca^{2+}. The analysis of the PDOS of spodumene (110) surface indicated that the activities of Li and Al on spodumene surface were too weak to act as active sites for the absorption of anionic collectors. The adsorption energy of Fe^{3+} on spodumene surface was calculated as -369.00 kJ/mol which is much greater than that of Ca^{2+}, i.e. -187.14 kJ /mol. This showed that Fe^{3+} is more apt to be adsorbed on spodumene surface than Ca^{2+} is.

The bond population in Ca-O was very low which indicated that the covalent proportion of the bond was very weak and ionic component existed in Ca-O bond. The bond population in Fe-O was high, illustrating that a covalent bond of Fe-O is formed. The PDOS of free Ca/Fe and the reacted O atom on spodumene (110) surface before and after the adsorption showed that the peaks of Fe 3d orbital and O 2p orbital overlapped at the Fermi level (E_f = 0) after the adsorption, implying a strong hybridization between them is formed. The DOS near the Fermi level of spodumene surface implied that the activity of the adsorbed Fe^{3+} on the mineral surface was greater than that of Ca^{2+}.

Acknowledgements

This research was funded by National Science and Technology Support program of the People's Republic of China (No. 2012BAB10B02). The authors are thankful for this support.

References

BLOSS F.D., 1971, *Crystallography and Crystal Chemistry*, Holt, Rinehart and Winston, New York.

BRAGG L., CLARINGBULL G.F., 1965, *Crystal Structures of Minerals*, G. Bell and Sons, London.

BURNS L., NELSON P.A., 1978, *Advanced batteries for vehicle propulsion*, Technical Paper Series, vol. 780458, Society of Automative Engineers, Warrendale.

COOPER J.F., BORG I.Y., O'CONNEL, L.G., BEHRIN E., RUBIN B., WIESNER H.J., 1976, *Lithium requirements for electric vehicles using lithium–water–air batteries.* In: Vine, J.D. (Eds.), Lithium Resources and Requirements by the Year 2000, Geological Survey Professional Paper, vol. 1005, U.S. Government Printing Office, Washington, 9-12.

FUERSTENAU D W, PRADIP, 2005, *Zeta potentials in the flotation of oxide and silicate minerals*, Advances in Colloid and Interface Science, 114–115, 9-26.

JOAN R., CLARK, ET AL., 1969, Crystal-chemical characterization of clinopyroxenes based on eight new structure refinements, Mineral. Soc. Amer. Spec. Pap., 2, 31-50.

KAZUME N., MASAHITO Y., MASAYUKI H., Energetics of Mg and B adsorption on polar zinc oxide surfaces from first principles, Phys. Rev. B, 2008, 77, 35330-35336.

KRAUSE J. T., 1968, *Internal Friction of Twinned Spodumene*, J. Appl. Phys., 39, 44-72.

KWANG SOON MOON, DOUGLAS W. FUERSTENAU, 2003, Surface crystal chemistry in selective flotation of spodumene (LiAl[SiO3]2) from other aluminosilicates, Int. J. Miner. Process., 72, 11-24.

LANDGREBE A.A., NELSON P.A., 1976, *Battery research sponsored by the U.S. energy research and development administration*, In: Vine, J.D. (Eds.), Lithium Resources and Requirements by the Year 2000, Geological Survey Professional Paper, vol. 1005, U.S. Government Printing Office, Washington, 2-5.

MONKHORST H.J., PACK J.D., 1976, *Special points for Brillouin-zone integrations*, Physical Review B, 13, 5188-5192.

NICHOLSON P., 1978, *Past and future development of the market for lithium in the world aluminum industry*, The International Journal of Energy, 3, 235-413.

PAYNE M.C., TETER M.P., ALLAN D.C., ARIAS T.A., JOANNOPOULOS J.D., 1992, *Iterative minimization techniques for ab initio total energy calculation: molecular dynamics and conjugate gradients*. Reviews of Modern Physics, 64, 1045-1097.

PENG WENSHI, LIU GAOKUI, 1982, *Atlas of mineral infrared spectroscopy*, Science Press, Beijing.

PERDEW J.P., BURKE K., ERNZERHOF M., 1996, *Generalized gradient approximation made simple*, Physical Review Letter, 77, 3865-3868.

PERDEW J.P., WANG Y., 1992, *Accurate and simple analytic representation of the electron-gas correlation energy*, Physical Review B, 45, 13244-13249.

REUTER K., SCHEFFLER M., *Composition, structure, and stability of RuO2(110) as a function of oxygen pressure*, Phys. Rev. B, 2001, 65, 035406-035417.

SEGALL M D, SHAH R, PICKARD C J, PAYNE M C, 1996, *Population analysis in plane wave electronic structure calculations*, Molecular Physics, 89, 571-577.

SUN CHUANYAO, YIN WANZHONG, 2001, *Difference in Floatability of Spodumene and Aegirine from the Same Ore Body*, Journal of China University of Mining & Technology, Vol. 30, 531-536.

VANDERBILT D., 1990, *Soft self-consistent pseudopotentials in a generalized eigenvalue formalism*, Physical Review B, 41, 7892-7895.

VON OERTZEN G.U., SKINNER W.M., NESBITT H.W., PRATT A.R., BUCKLEY A.N., 2007, *Cu adsorption on pyrite (100): ab initio and spectroscopic studies*, Surface Science, 601, 5794-5799.

WENDT G., 1971, *Operating experiences with electrolytes containing lithium fluoride*, *Metallurgical Transactions*, 2, 155-161.

ZACHARIASEN W.H., 1963, *The crystal structure of monoclinic metaboric acid*, Acta Crystallographica, 16, 385-392.